

MeteorPred: A Meteorological Multimodal Large Model and Dataset for Severe Weather Event Prediction

Shuo Tang^{1,2,3}, Jian Xu^{1,2}, Jiadong Zhang^{1,2,3}, Yi Chen^{1,2,3}, Qizhao Jin⁴, Lingdong Shen^{1,2},
Chenglin Liu^{1,2,3}, Shiming Xiang^{1,2}

¹MAIS, Institute of Automation, Chinese Academy of Sciences

²School of Artificial Intelligence, University of Chinese Academy of Sciences

³Zhongguancun Academy, Beijing

⁴China Meteorological Administration

tangshuo2024@ia.ac.cn, jian.xu@ia.ac.cn

Abstract

Timely and accurate severe weather warnings are critical for disaster mitigation. However, current forecasting systems remain heavily reliant on manual expert interpretation, introducing subjectivity and significant operational burdens. With the rapid development of AI technologies, the end-to-end “AI weather station” is gradually emerging as a new trend in predicting severe weather events. Three core challenges impede the development of end-to-end AI severe weather system: (1) scarcity of severe weather event samples; (2) imperfect alignment between high-dimensional meteorological data and textual warnings; (3) existing multimodal language models are unable to handle high-dimensional meteorological data and struggle to fully capture the complex dependencies across temporal sequences, vertical pressure levels, and spatial dimensions. To address these challenges, we introduce MP-Bench, the first large-scale temporal multimodal dataset for severe weather events prediction, comprising 421,363 pairs of raw multi-year meteorological data and corresponding text caption, covering a wide range of severe weather scenarios across China. On top of this dataset, we develop a meteorology multimodal large model (MMLM) that directly ingests 4D meteorological inputs. In addition, it is designed to accommodate the unique characteristics of 4D meteorological data flow, incorporating three plug-and-play adaptive fusion modules that enable dynamic feature extraction and integration across temporal sequences, vertical pressure layers, and spatial dimensions. Extensive experiments on MP-Bench demonstrate that MMLM performs exceptionally well across multiple tasks, highlighting its effectiveness in severe weather understanding and marking a key step toward realizing automated, AI-driven weather forecasting systems. Our source code and dataset will be made publicly available.

Introduction

Severe weather events, including rain storm, snow storm, hail, gale, frost, heat wave, cold wave, and other high-impact atmospheric phenomena, are occurring with increasing frequency (Hoeppe 2016; Stephenson, Diaz, and Mur-nane 2008). These hazards impose escalating strains worldwide on transportation systems (Liu et al. 2023), energy infrastructure (Perera et al. 2020), agricultural production (Lesk, Rowhani, and Ramankutty 2016), and public safety (Liao et al. 2025). Consequently, timely and accurate forecasts are critical for effective emergency response and dis-

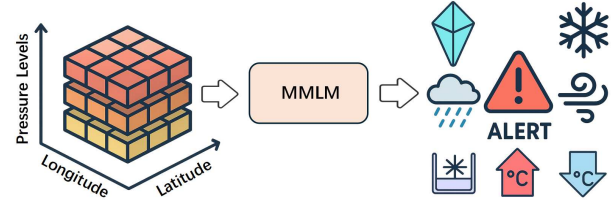


Figure 1: Conceptual illustration for severe weather event prediction using the Meteorological Multimodal Large Model (MMLM).

aster mitigation, supporting vital decision-making in public safety, transportation, and industrial production. The meteorological variables in severe weather are complex and variable in their spatial and temporal distribution. Currently, severe weather warnings have to follow a rigorous process. First, the source data observed from satellites, radar and ground stations are assimilated into Numerical Weather Prediction (NWP) systems (Bauer, Thorpe, and Brunet 2015) and modern AI-based forecasting models for weather prediction (Chen et al. 2023; Price et al. 2025). Then, operational forecasters analyze comprehensively the output of the models and correct the details to formally release the warnings to the public. However, manually interpreting, drafting, and reviewing forecasts is not only time-consuming but also heavily dependent on the forecaster’s expertise and subjective judgment, inevitably increasing the risk of oversight (American Meteorological Society 2021). This challenge makes the development of an AI-driven severe weather warning system essential—a system that ingests the latest NWP output, instantly produces accurate warnings, and provides continuously rolling updates, representing the future of severe weather forecasting through a fully automated early-warning pipeline. (Reichstein et al. 2025).

The development of end-to-end AI-based severe weather systems (as shown in Fig. 1) is currently hindered by three major challenges. First, existing severe weather datasets are often small-scale, event-specific, or geographically and temporally limited, making it difficult to train and evaluate models with strong generalization capabilities (Kafi and Ponrahono 2024; Olivetti and Messori 2024). Second, the alignment between high-dimensional meteorological data and

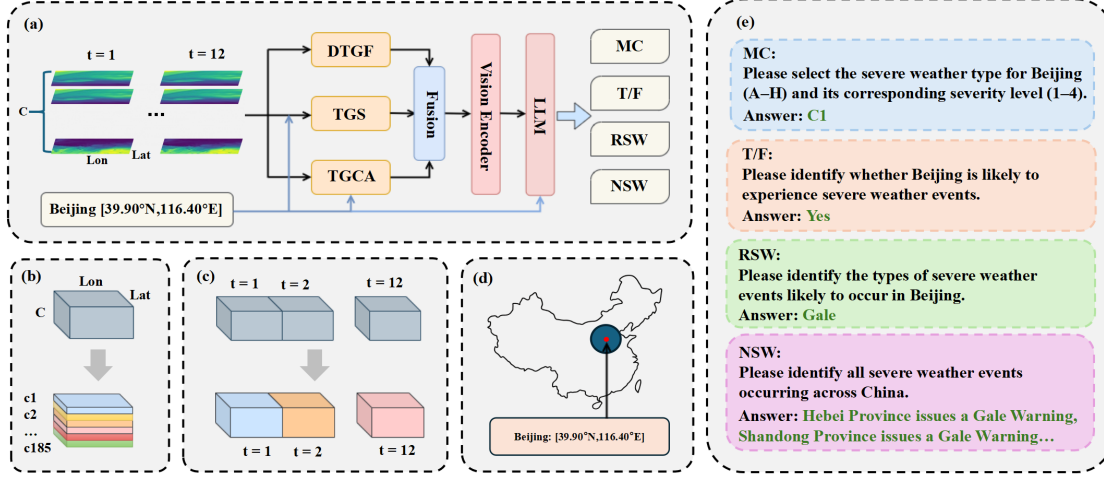


Figure 2: Overview of the MMLM framework and its core components. (a) Displays the MMLM architecture; (b), (c), and (d) illustrate the three proposed plug-and-play modules TGF, GCA, and TGS, respectively, with (e) showcasing four QA samples from MP-Bench.

textual descriptions of severe weather events remains imperfect, and compressing meteorological data into daily averages further reduces temporal resolution, impairing the ability to capture rapid or dramatic atmospheric changes on short time scales. Third, there is no existing multimodal large language model (MLLM) that can handle the raw meteorological data well. Consequently, for the gridded data of vertical pressure layers obtained at each moment, most previous methods manually select a subset to adapt to the input requirements of existing encoders. This over-simplification discards critical information, such as vertical structure, temporal dynamics, and inter-variable physical relationships, leading to a significant degradation in prediction accuracy. Moreover, 4D gridded data (time \times pressure level \times longitude \times latitude) are often flattened or projected into two-dimensional visual formats, which hinders MLLMs from capturing the intrinsic physical dependencies and spatiotemporal evolution of atmospheric systems.

To address these challenges, we present a unified framework consisting of a large-scale benchmark dataset and a meteorology multimodal large model. Specifically, we constructed a brand new dataset, MP-Bench, which is a nationwide, year-round coverage severe weather events dataset. It contains 421,363 data pairs, including rain storm, snow storm, hail, gale, frost, heat wave, cold wave and normal weather samples. Using each warning’s issuance time as the reference point, we collect the national multi-variable meteorological fields for the next 12 hours and pair them with that the warning to ensure precise cross-modal temporal alignment. In order to fully demonstrate the language comprehension capability and application potential of MLLM, we constructed four types of QA pairs, including **Multiple Choice Questions**, **True/False Questions**, **RSW Questions** and **NSW Questions**. With this work setting, it is hoped to enrich the downstream task scenarios.

On this data foundation, we develop MMLM, a multimodal model tailored for 4D meteorological data. The

model integrates three plug-and-play functional modules—the Dynamic Temporal Gating Fusion (DTGF) module, the Text-Driven Gaussian Spatial Masking (TGS) module, and the Text-Driven Channel Attention (TGCA) module, specifically designed to enhance feature extraction along the temporal, spatial, and vertical dimensions, respectively. The synergistic interaction among these modules significantly improves MMLM’s capacity to capture and interpret complex multidimensional meteorological patterns.

Our contributions could be summarized as:

- We have collected MP-Bench, a dataset for severe weather events prediction that provides nationwide scope, year-round coverage, and a rich variety of Q&A formats.
- Based on this dataset, we proposed MMLM, integrating three plug-and-play modules that enhance feature extraction in temporal, spatial, and vertical dimensions, respectively, collectively improving its ability to capture complex meteorological patterns.
- To the best of our knowledge, this is the first time that MLLM has been used to deeply interpret raw meteorological data and generate warning conclusions in sentence form, paving a whole new perspective for future severe weather warning missions.

Related Works

Severe Weather Event Prediction

Current approaches for AI-based severe weather event prediction can be broadly categorized into three main paradigms: gridded meteorological data-driven base models, intelligent inference methods leveraging LLMs, and end-to-end prediction frameworks based on MLLMs that integrate data from diverse sources.

There are well-established works that leverage gridded meteorological data to drive base models (Lam et al. 2023;

Dataset	Meteorological Variables	Text Events	Severe Weather Types
CrisisLex (Olteanu et al. 2014)	×	2,840,000	2
ClimaBench (Laud et al. 2023)	×	37,989	6
Climate-FEVER (Diggelmann et al. 2020)	×	1,535	5
GridRad-Severe (Murphy, Homeyer, and Allen 2023)	Remote Sensing	×	3
SEVIR (Veillette, Samsi, and Mattioli 2020)	Remote Sensing	×	5
HR-Extreme (Ran et al. 2024)	NWP	×	5
WeatherQA (Ma et al. 2024)	Reanalysis, Observation	8,000	5
ClimateIQA (Chen et al. 2024a)	Reanalysis	762,120	1
CLLMate (Li et al. 2024)	Reanalysis	41,000	3
OmniEarth-Bench (Wang et al. 2025a)	Remote Sensing	6,395	5
MP-Bench	Reanalysis	421,363	7

Table 1: Comparison between MP-Bench and existing datasets. The number of severe weather categories is consolidated based on primary meteorological elements.

Bi et al. 2023; Ravuri et al. 2021; Wu et al. 2023; Xiao et al. 2023; Gan et al. 2025), which directly predict the spatial distributions of meteorological variables at the next time step. However, these approaches do not incorporate high-level semantic representations of discrete severe weather phenomena, thereby limiting their capacity to produce intuitive and actionable warnings.

Some studies LLMs with retrieval-augmented generation (RAG) frameworks (Martelo, Ahmadiyehyazdi, and Wang 2024; Wang et al. 2025b; Li et al. 2025; Wang et al. 2025a), compressing high-dimensional gridded meteorological data into daily mean variables through spatial aggregation and temporal averaging while extracting structured semantics to generate expert-level analysis reports. However, this approach neglects the physical laws governing high-dimensional meteorological field evolution, limits its ability to capture complex dynamic changes, and leaves the LLMs susceptible to hallucinations.

The rapid development of MLLMs has opened up new research perspectives for severe weather prediction (Chen et al. 2024a; Ma et al. 2024; Li et al. 2024; Wang et al. 2025a; Bodnar et al. 2025). These studies encode high-dimensional meteorological or environmental data into three channels and incorporate corresponding textual information as input to MLLMs, enabling visual question answering and complex reasoning over severe weather or environmental events. However, such methods still have limitations on data processing. To align meteorological data with textual event records, complex meteorological fields are often compressed into daily averages, resulting in coarse temporal resolution and impairing the ability to capture rapid or dramatic atmospheric changes on short time scales. Meanwhile, to fit the input requirements of MLLMs, only variables from a few pressure levels are selected and temporally averaged, then compressed into RGB images, a process that may discard critical spatiotemporal information.

Related Datasets

From the comparison (As shown in Table 1), these datasets are leveraged to develop more robust language models for severe weather understanding. CrisisLex (Olteanu et al. 2014), ClimaBench (Laud et al. 2023), and Climate-FEVER (Diggelmann et al. 2020) each address language understand-

ing tasks centered on severe weather, including information filtering, reasoning, and scientific claim verification. However, all three datasets rely solely on textual data, and the lack of integration with meteorological modalities limits their ability to capture the full meteorological context and physical grounding of severe weather events.

SEVIR (Veillette, Samsi, and Mattioli 2020) and GridRad-Severe (Murphy, Homeyer, and Allen 2023) are datasets derived from remote sensing data, specifically designed to facilitate the detection, classification, and predictive modeling of severe weather events. HR-Extreme (Ran et al. 2024) leverages high-resolution numerical weather prediction data to support research on the spatiotemporal detection and classification of diverse severe weather phenomena. However, relying solely on meteorological data for severe weather forecasting has significant limitations. These datasets often lack semantic interpretability, making them difficult to use directly for issuing warnings.

OmniEarth-Bench (Wang et al. 2025a), ClimateIQA (Chen et al. 2024a), WeatherQA (Ma et al. 2024) and CLLMate (Li et al. 2024) represent multimodal datasets focused on severe weather phenomena and have demonstrated efficacy in severe weather event prediction tasks. However, no existing dataset concurrently provides large-scale textual warnings with comprehensive coverage across diverse severe weather types.

We present MP-Bench, a large-scale multimodal dataset built upon years of severe weather event forecasts. Unlike prior works, it integrates 421,363 textual warnings accumulated nationwide from meteorological stations over multiple years, covering seven typical categories of severe weather while preserving the original temporal information of meteorological data. This establishes a robust foundation for severe weather prediction with large-scale data, broad category coverage, and meteorological feature integrity.

MP-Bench

Dataset Overview

Data Source The dataset used in this study is comprised of two components: gridded meteorological data (ERA5) (Hersbach et al. 2020) and a textual dataset of severe weather events. ERA5, developed by the European Centre for Medium-Range Weather Forecasts (ECMWF), is a

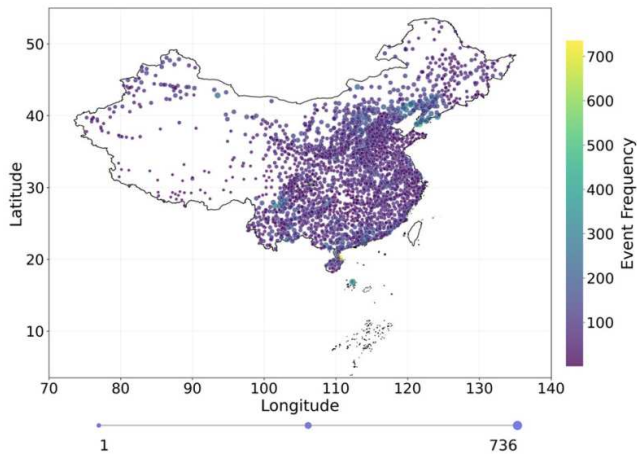


Figure 3: Spatial distribution of severe weather events across China. Symbol size corresponds to regional severe weather frequency.

global atmospheric reanalysis dataset. It offers a comprehensive range of meteorological variables with an hourly temporal resolution, covering both land and ocean regions globally at a spatial resolution of 0.25° in latitude and longitude. Additionally, it includes 37 vertical pressure levels ranging from 1000 hPa to 1 hPa, enabling a detailed representation of atmospheric thermal and dynamic processes from the troposphere up to the top of the stratosphere. In this study, we focus specifically on the region of China. The selected variables include temperature, humidity, precipitation, wind speed, and pressure. Each variable is represented across all 37 vertical pressure levels, which are treated as separate channels in our data structure. The data are sampled at multiple time steps, resulting in a four-dimensional format: (time \times pressure level \times longitude \times latitude).

The severe weather event text data were obtained from the China Meteorological Administration (CMA), which provides daily rolling updates of severe weather warnings issued by regional meteorological stations nationwide. The collected data include records from the years 2023 and 2024, covering 2,412 regional weather stations across China. To focus on the most prevalent types of severe weather, we filtered the dataset to include seven representative categories of severe weather warning events for further analysis: rainstorm, snowstorm, gale, cold wave, heat wave, frost, and hail. To maintain consistency in labeling, only the issuance time, geographic location, event type, and severity level are retained from each warning. Each warning record indicates that the specified type of severe weather is expected to occur in the associated region within the next few hours. After data cleaning, a total of 371,703 valid warning records were obtained, and the distribution of records and their categories is presented in Fig. 3. Detailed data distribution is provided in the appendix. To alleviate category imbalance and enhance the model’s discriminative capability, we sampled “normal weather” entries evenly across regions and seasons, resulting in an additional 49,660 negative samples. In total, the dataset comprises 421,363 entries.

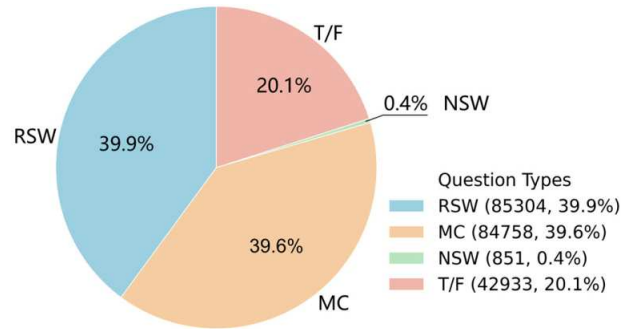


Figure 4: Proportional distribution of the four QA question types (2023).

Data Alignment Accurately aligning high-dimensional gridded meteorological data with warning issuance times has always been challenging. To preserve the original temporal and 3D spatial information in ERA5, we have deviated from previous approaches by avoiding temporal averaging. Instead, we have extracted a 12-hour window spanning $[t, t+11]$ hours starting at the warning issuance time t , enabling precise alignment of meteorological data with textual events on the time axis.

QA pairs To better fulfill practical application requirements, we designed four distinct types of QA tasks, including Multiple Choice Questions, True/False Questions, RSW Questions and NSW Questions. Fig. 4 illustrates the proportional distribution of these task categories. These task types differ in terms of spatial granularity, ranging from regional levels (e.g., provinces, cities, and counties in China) to the national scale, as well as in the level of detail required for querying severe weather events—specifically, whether the query pertains solely to the type of weather event or includes both the type and its severity level. We employ 2023 data as the training set and a subset of 2024 data as the test set.

Multiple Choice Questions (MC): These questions are specifically designed to enable fine-grained identification of severe weather events in a given region. Based on the classification criteria for severe weather issued CMA, we categorize severe weather into seven primary types (A–G), with an additional option representing normal weather conditions (H). Each primary category is further subdivided into two to four subcategories based on the severity level of the event (e.g., A.1 denotes a blue rainstorm warning). Each question includes multiple alternative options, from which the model is required to select the single answer that best aligns with the provided meteorological data and the query.

True/False Questions (T/F): These questions are used to determine whether severe weather is occurring in a specified region, with “Yes” or “No” as the possible responses. The model analyzes the gridded meteorological data and integrates it with the user-defined geographic area to assess whether the region is under severe weather conditions during the target time period.

RSW Questions: These questions are designed to evaluate the model’s ability to identify types of severe weather in specific region. Given a location specified in the query,

Category	Model	MC-main \uparrow	MC-sub \uparrow	T/F \uparrow	RSW \uparrow	NSW \uparrow
Closed-source	GPT-4o	11.92	6.51	0.19	14.03	0.1
Open-source	LLaVA-NeXT-Video-7B	47.74	37.54	79.39	41.14	0.7
	Video-LLaVA-7B	52.12	42.43	78.67	47.27	1.7
	InternVL3-8B	58.31	47.03	79.40	39.10	1.9
	Qwen2.5-VL-7B-Instruct	72.37	58.19	87.13	67.46	2.1

Table 2: Performance comparison of MMLMs and closed-source model on MP-Bench. All open-source models are enhanced with three plug-and-play modules (DTGF, TGS, and TGCA). Scoring scales: First Four Entries (0-100); Last Entry (0-5).

the model analyzes the corresponding meteorological data to determine the occurrence of severe weather. If no severe weather is detected, “no severe weather” is returned to ensure format consistency and evaluation reliability.

NSW Questions evaluates the model’s ability to understand and describe nationwide severe weather conditions for a given date. Based on the meteorological data, the model must generate a structured natural language response listing all severe weather events in the form of *[geographic name][weather type][severity level]*. To ensure high-quality evaluation, we developed a fine-grained scoring criterion and employed GPT-4o for automated semantic scoring, considering completeness, accuracy, and expression quality.

Meteorological Multimodal Large Model

The proposed Meteorological Multimodal Large Model (MMLM) incorporates three plug-and-play modules: the Dynamic Time-Gated Fusion (DTGF) module, the Text-Driven Gaussian Spatial Masking (TGS) module, and the Text-Driven Channel Attention (TGCA) module. Depicted in Fig. 2, the meteorological data are processed in parallel through three distinct modules. Their outputs are concatenated, fused via a 3D convolutional layer, and then mapped to the input dimensionality of the baseline model through an MLP. The resulting features are fed into an LLM to generate textual warnings for severe weather events.

DTGF

To better identify spatiotemporal regions with abrupt or substantial changes in the meteorological field, we employ the DTGF module, which dynamically generates gating based on the differences in meteorological data between adjacent time steps and performs weighted fusion of temporal tokens. The module can be formulated as follows:

$$\Delta \mathbf{x}_t = \|\mathbf{x}_t - \mathbf{x}_{t-1}\|_2, \quad t = 2, \dots, T \quad (1)$$

$$g_t = \sigma(\text{MLP}(\Delta \mathbf{x}_t)), \quad g_t \in [0, 1] \quad (2)$$

$$\tilde{\mathbf{x}}_t = g_t \cdot \mathbf{x}_t. \quad (3)$$

where $\mathbf{x}_t \in \mathbb{R}^{T \times C \times H \times W}$ represent ERA5 data. $\Delta \mathbf{x}_t$ is the L2-norm of adjacent hour data. The g_t represents gating weight, and $\tilde{\mathbf{x}}_t$ represents the weighted meteorological features.

TGS

To guide the model to focus on the geographic locations specified in the textual input, we propose TGS module. This module maps the geographic coordinates (ϕ_i, λ_i) extracted from text events onto the gridded meteorological data, generates a 2D Gaussian weight mask around each point, and weights the spatial features of each channel and time step to enhance the model’s attention on those regions. The module performs the following operations:

$$(\phi_i, \lambda_i) \rightarrow (u_i, v_i), \quad i = 1, \dots, N_{\text{coord}} \quad (4)$$

$$G(u, v) = \exp\left(-\frac{(u - u_j)^2 + (v - v_j)^2}{2\sigma^2}\right), \quad (5)$$

$$j = 1, \dots, N_{\text{ERA5}}$$

$$M(u, v) = \sum_{i=1}^{N_{\text{coord}}} G_j(u_i, v_i). \quad (6)$$

where (u_i, v_i) denote the latitude/longitude of grid points in ERA5 data. $G_i(u, v)$ computes Gaussian weights based on the distance between textual locations and weather grid points. $M(u, v)$ represents the sum of Gaussian weight masks corresponding to all coordinates extracted from the text-based weather warnings.

TGCA

Since each weather element includes 37 pressure-level channels in the vertical dimension, the aggregation of 185 input channels from the five elements introduces a significant amount of redundancy. To better leverage this high-dimensional information, we propose the TGCA, which dynamically generates attention weights for each weather channel and re-weights the original spatiotemporal features based on the similarity between the input text and channel descriptions. The module can be formulated as follows:

$$\mathbf{P} = \text{Linear}(\mathbf{y}), \quad (7)$$

$$\mathbf{v} = \text{Mean}(\mathbf{x}), \quad (8)$$

$$\mathbf{Y} = \mathbf{X} \cdot \sigma(\text{Softmax}(\mathbf{v} \mathbf{P}^\top) \mathbf{P}). \quad (9)$$

where $\mathbf{y} \in \mathbb{R}^{B \times L \times D}$ denotes text embeddings of length L with dimension D . \mathbf{P} projects text embeddings to the channel dimension via learnable linear layer $\text{Linear} : \mathbb{R}^D \rightarrow \mathbb{R}^C$. \mathbf{v} computes channel-wise descriptors by spatiotemporal averaging (excluding channel dimensions). \mathbf{Y} represents the channel-weighted ERA5 features.

Experiments

Experimental Settings

All experiments were carried out on a distributed cluster of eight NVIDIA A800 GPUs (40GB) for both training and evaluation. We selected four baseline models, namely Qwen2.5-VL-7B-Instruct (Bai et al. 2025), LLaVA-NeXT-Video-7B (Zhang et al. 2024), Video-LLaVA-7B (Lin et al. 2023), and InternVL3-8B (Chen et al. 2024b), and integrated three plug-and-play modules (DTGF, TGS, and TGCA) for fine-tuning and evaluation. All models were fine-tuned with LoRA (rank = 8, $\alpha = 16$) applied to both attention weights and the added modules, using a learning rate of 5×10^{-5} , batch size 2, gradient accumulation over 8 steps, and bf16 precision. More details were provided in the appendix.

Evaluation Metrics

For MC Questions, the model had to select the correct answer from four options; for T/F Questions, it had to provide the correct judgment; and for RSW Questions, the model was required to select one of eight weather categories, including rain storm, snow storm, gale, cold wave, heat wave, frost, hail, and normal weather. The accuracy of these responses was calculated and scaled to a maximum of 100. NSW Questions were scored by GPT on a 0–5 scale (criteria in the appendix), and the final composite score was the mean across all samples.

Closed-Source Model Performance Evaluation

In this section, we selected GPT-4o as a representative closed-source model and systematically evaluated its performance in severe weather forecasting to establish the critical necessity of the proposed MMLM. Inspired by the CLL-Mate, this study selected four key meteorological variables, including 2-meter temperature, 10-meter u-component of wind, 10-meter v-component of wind, and total precipitation—and vectorially synthesized the u/v wind components into a unified wind field to construct a three-channel meteorological input compatible with GPT-4o’s requirements. Concurrently, ERA5 reanalysis data from 12 hours post-severe weather warning issuance were spatiotemporally matched with corresponding warning texts. Experimental results (as show in Table 2) demonstrated that GPT-4o exhibits severely limited performance across all tasks, with critically low accuracy in T/F, RSW, and NSW tasks, confirming its inability to effectively handle meteorological question answering.

Quantitative Results Analysis

Performance Improvement over Closed-Source Model

The results for the four baseline models were summarised in Table 2. Compared with the closed-source baseline, our method yielded substantial gains on every task. On MC-main, the accuracy ranged from 47.74% to 72.37%, representing an improvement of approximately 35-60%, indicating the model can reliably identify both the type and severity level of severe weather. T/F accuracy improves by 79-87%, confirming the model’s effectiveness in predicting whether an extreme event will occur, while RSW accuracy rises by

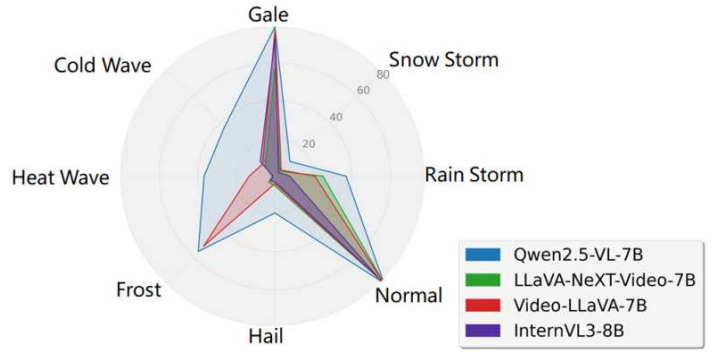


Figure 5: Accuracy scores of different MMLMs across diverse severe weather types.

25-53%. By contrast, the NSW score remains at only 2.1%, underscoring the intrinsic difficulty of this task despite the marked improvement over the closed-source model.

Performance Comparison of MMLMs These results showed that Qwen2.5-VL-based MMLM achieved the best performance across all the QA tasks. Specifically, by leveraging 2D-RoPE and a windowed attention mechanism, the model delivered superior spatiotemporal encoding and processed high-resolution meteorological data efficiently without compromising computational efficiency. This capability, combined with its robust pretrained language backbone ensured precise alignment between textual queries and meteorological visual features, thereby boosting overall accuracy. It also demonstrated greater compatibility with—and larger performance gains from—the three plug-and-play modules (DTGF, TGS, and TGCA).

Weather Type Analysis As shown in Fig. 5, the average accuracy across eight weather types exhibited significant variations: all models consistently achieved prediction accuracy above 80% for gale events and normal weather conditions, while snow storm prediction accuracy was the lowest ($\leq 6\%$). This discrepancy stemmed primarily from severe dataset imbalance—the snow storm samples accounted for only 1.7% of the training data, making it difficult for models to adequately model the complex microphysical processes characteristic of winter storms. Notably, the Qwen2.5-VL-based and Video-LLaVA-based MMLMs demonstrated significant advantages in frost prediction, with accuracies reaching 56.32% and 52.45%, respectively, which were 50% higher than those of the other models. Crucially, the Qwen2.5-VL-based MMLM outperformed the other three models across all eight weather types, and its performance advantage validated the model’s unified spatiotemporal reasoning capability.

Ablation Study

To further assess the effectiveness of the three plug-and-play modules (DTGF, TGS, and TGCA), we randomly sampled 5,000 instances from the MP-Bench dataset while maintaining the same proportions of severe-weather types and QA categories as in the training set. Quantitative results in Table 3 illustrate that:

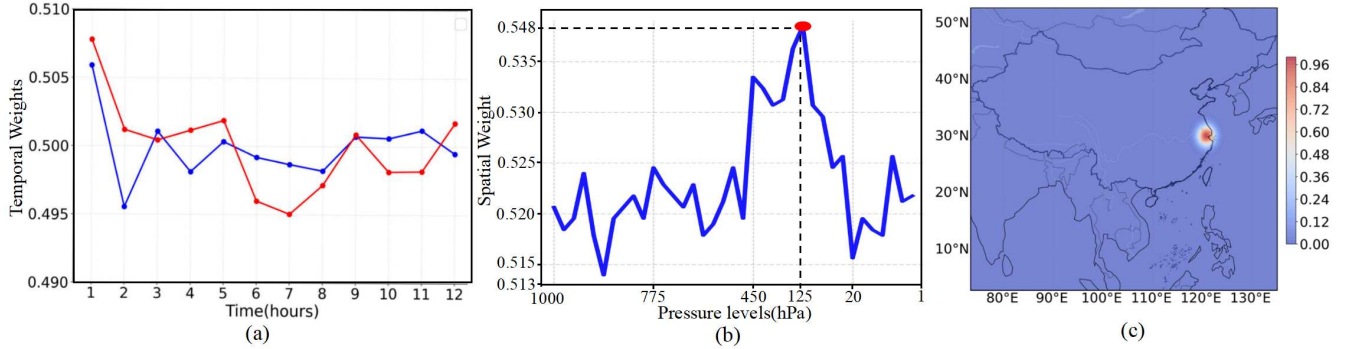


Figure 6: Weight distribution patterns of three types of plug-and-play modules: (a)DTGF, (b) TGCA, (c) TGS. Additional examples are in appendix.

Baseline(Qwen2.5-VL-7B-Instruct)			Evaluation Metrics				
DTGF	TGS	TGCA	MC-main \uparrow	MC-sub \uparrow	T/F \uparrow	RSW \uparrow	NSW \uparrow
×	×	×	42.73	28.01	58.47	41.25	1.1
✓	×	×	53.28	34.84	57.23	47.30	1.2
×	✓	×	44.57	29.66	54.81	41.92	1.2
×	×	✓	50.91	34.62	60.35	50.29	1.4
✓	✓	×	53.81	32.02	56.63	54.02	1.4
✓	×	✓	50.93	32.61	67.17	51.87	1.3
×	✓	✓	51.97	31.99	70.44	57.23	1.4
✓	✓	✓	57.23	36.01	79.21	58.63	1.7

Table 3: Ablation study of the three proposed plug-and-play modules in MMLM.

DTGF significantly enhances model’s temporal feature extraction ability. With the DTGF module operating in standalone mode, the model achieved significant improvement in MC questions aimed at identifying severe weather types and severity levels. Fig. 6 (a) displayed the temporal weight distributions for blue and red warnings. For red warnings, the module assigned higher weights to the first three hours after issuance than to other periods, consistent with the physical evolution of meteorological fields (verified in the appendix). This indicated that the module could effectively focus on meteorological information during critical time windows, thereby improving the accuracy of severe weather forecasts.

TGS improves the model’s focus on the geographic area specified by the text. Fig. 6 (c) visually demonstrated the Gaussian weight distribution of the TGS module, revealing that the model precisely focused on regions specified in queries. When TGS and DTGF were combined, they significantly improved performance on both MC-main and RSW, confirming the complementary nature of their features.

TGCA filters redundant channels to allow models to understand the meteorological factors that influence severe weather. When the TGCA module was introduced, T/F metrics showed significant improvement, with the TGCA-TGS combination yielding the highest gain (7.25%). Additionally, we visualized the 37-channel weight distributions for five meteorological variables (temperature, humidity, precipitation, wind speed, and pressure). Using radial wind speed in Fig. 6 (b) as an example, the wind speed weight at

125 hPa was significantly higher than at other layers, indicating its key role in extreme weather prediction. Channel weight distributions for the remaining four variables were detailed in the appendix.

The parallel fusion of three modules achieves optimal performance. DTGF’s temporal highlighting compensated for TGCA’s channel pruning, while TGS spatial masks focused computations exclusively on high-risk regions. The 36.01% overall gain in MC-sub confirmed the modules’ distinctly complementary functional roles and proved the effectiveness of the parallel module strategy.

Conclusion

AI-driven severe weather prediction has shown great potential. In this study, we have collected the MP-Bench dataset, thereby addressing the scarcity of data for severe weather forecasting and introducing a more precise alignment strategy between meteorological grids and textual warnings. Building on this foundation, we have developed a Meteorological Multimodal Large Model (MMLM) and have integrated three plug-and-play modules into its architecture, markedly enhancing the model’s ability to capture spatiotemporal patterns and vertical pressure-level information.

Nevertheless, analysis reveals that model-misclassified samples exhibit more complex meteorological field characteristics (as verified in the appendix). Integrating physical constraints with multi-source data could enhance forecasting accuracy for complex meteorological fields.

References

- American Meteorological Society. 2021. Weather Analysis and Forecasting: An Information Statement of the American Meteorological Society. Information Statement, American Meteorological Society. Adopted by the AMS Council on 20 December 2021.
- Bai, S.; Chen, K.; Liu, X.; Wang, J.; Ge, W.; Song, S.; Dang, K.; Wang, P.; Wang, S.; Tang, J.; et al. 2025. Qwen2.5-VL Technical Report. *arXiv preprint arXiv:2502.13923*.
- Bauer, P.; Thorpe, A.; and Brunet, G. 2015. The quiet revolution of numerical weather prediction. *Nature*, 525(7567): 47–55.
- Bi, K.; Xie, L.; Zhang, H.; Chen, X.; Gu, X.; and Tian, Q. 2023. Accurate medium-range global weather forecasting with 3D neural networks. *Nature*, 619(7970): 533–538.
- Bodnar, C.; Bruinsma, W. P.; Lucic, A.; Stanley, M.; Allen, A.; Brandstetter, J.; Garvan, P.; Riechert, M.; Weyn, J. A.; Dong, H.; Gupta, J. K.; Thambiratnam, K.; Archibald, A. T.; Wu, C.-C.; Heider, E.; Welling, M.; Turner, R. E.; and Perdikaris, P. 2025. A foundation model for the Earth system. *Nature*, 641(8065): 1180–1187.
- Chen, J.; Zhou, P.; Hua, Y.; Chong, D.; Cao, M.; Li, Y.; Yuan, Z.; Zhu, B.; and Liang, J. 2024a. Vision-Language Models Meet Meteorology: Developing Models for Extreme Weather Events Detection with Heatmaps. *arXiv preprint arXiv:2406.09838*.
- Chen, L.; Zhong, X.; Zhang, F.; Cheng, Y.; Xu, Y.; Qi, Y.; and Li, H. 2023. FuXi: a cascade machine learning forecasting system for 15-day global weather forecast. *npj Climate and Atmospheric Science*, 6(1): 190.
- Chen, Z.; Wu, J.; Wang, W.; Su, W.; Chen, G.; Xing, S.; Zhong, M.; Zhang, Q.; Zhu, X.; Lu, L.; et al. 2024b. Internvl: Scaling up vision foundation models and aligning for generic visual-linguistic tasks. In *Proceedings of the IEEE/CVF Conference on Computer Vision and Pattern Recognition*, 24185–24198.
- Diggelmann, T.; Boyd-Graber, J.; Bulian, J.; Ciaramita, M.; and Leippold, M. 2020. CLIMATE-FEVER: A Dataset for Verification of Real-World Climate Claims. *Proceedings of the Tackling Climate Change with Machine Learning Workshop at NeurIPS 2020*, 1: 1–16.
- Gan, L.; Man, X.; Zhang, C.; and Shao, J. 2025. EW-MoE: An effective model for global weather forecasting with mixture-of-experts. In *Proceedings of the AAAI Conference on Artificial Intelligence*, volume 39, 210–218.
- Hersbach, H.; Bell, B.; Berrisford, P.; Hirahara, S.; Horányi, A.; Muñoz Sabater, J.; Nicolas, J.; Peubey, C.; Radu, R.; and Schepers, D. 2020. The ERA5 Global Reanalysis. *Quarterly Journal of the Royal Meteorological Society*, 146(730): 1999–2049.
- Hoeppe, P. 2016. Trends in Weather Related Disasters—Consequences for Insurers and Society. *Weather and Climate Extremes*, 11: 70–79.
- Kafi, K. M.; and Ponrahono, Z. 2024. Advances in weather and climate extreme studies: a systematic comparative review. *Discover Geoscience*, 2(1): 66.
- Lam, R.; Sanchez-Gonzalez, A.; Willson, M.; Wirnsberger, P.; Fortunato, M.; Alet, F.; Ravuri, S.; Ewalds, T.; Eaton-Rosen, Z.; Hu, W.; et al. 2023. Learning skillful medium-range global weather forecasting. *Science*, 382(6677): 1416–1421.
- Laud, T.; Spokoyny, D.; Corringham, T.; and Berg-Kirkpatrick, T. 2023. ClimaBench: A Benchmark Dataset for Climate Change Text Understanding in English. *CoRR*, abs/2301.04253: 1–15.
- Lesk, C.; Rowhani, P.; and Ramankutty, N. 2016. Influence of extreme weather disasters on global crop production. *Nature*, 529(7584): 84–87.
- Li, H.; Wang, Z.; Wang, J.; Wang, Y.; Lau, A.; and Qu, H. 2024. CLLMate: A Multimodal Benchmark for Weather and Climate Events Forecasting. *arXiv preprint arXiv:2409.19058*.
- Li, H.; Wong, K.; Luo, Y.; Chen, J.; Liu, C.; Zhang, Y.; Lau, A.; Qu, H.; and Liu, D. 2025. Save It for the “Hot” Day: An LLM-Empowered Visual Analytics System for Heat Risk Management. *IEEE Transactions on Visualization and Computer Graphics*.
- Liao, S.; Pan, W.; Wen, L.; chen, R.; Pan, D.; Wang, R.; Hu, C.; Duan, H.; Weng, H.; Tian, C.; Kong, W.; Jinghan, R.; Zhang, Y.; Xi, M.; Zhang, X.; and Wang, X. 2025. Temperature-Related Hospitalization Burden under Climate Change. *Nature*.
- Lin, B.; Ye, Y.; Zhu, B.; Cui, J.; Ning, M.; Jin, P.; and Yuan, L. 2023. Video-LLaVA: Learning United Visual Representation by Alignment Before Projection. *arXiv preprint arXiv:2311.10122*.
- Liu, K.; Wang, Q.; Wang, M.; and Koks, E. E. 2023. Global transportation infrastructure exposure to the change of precipitation in a warmer world. *Nature Communications*, 14(1): 2541.
- Ma, C.; Hua, Z.; Anderson-Frey, A.; Iyer, V.; Liu, X.; and Qin, L. 2024. WeatherQA: Can Multimodal Language Models Reason About Severe Weather? *arXiv preprint arXiv:2406.11217*.
- Martelo, R.; Ahmadiyehyazdi, K.; and Wang, R. 2024. Towards Democratized Flood Risk Management: An Advanced AI Assistant Enabled by GPT-4 for Enhanced Interpretability and Public Engagement. *arXiv preprint arXiv:2403.03188*.
- Murphy, A. M.; Homeyer, C. R.; and Allen, K. Q. 2023. Development and Investigation of GridRad-Severe, a Multi-year Severe Event Radar Dataset. *Monthly Weather Review*, 151(9): 2257 – 2277.
- Olivetti, L.; and Messori, G. 2024. Advances and prospects of deep learning for medium-range extreme weather forecasting. *Geoscientific Model Development*, 17(6): 2347–2358.
- Olteanu, A.; Castillo, C.; Diaz, F.; and Vieweg, S. 2014. Crisislex: A lexicon for collecting and filtering microblogged communications in crises. In *Proceedings of the international AAAI conference on web and social media*, volume 8, 376–385.
- Perera, A. T. D.; Nik, V. M.; Chen, D.; Scartezzini, J.-L.; and Hong, T. 2020. Quantifying the impacts of climate change and extreme climate events on energy systems. *Nature Energy*, 5(2): 150–159.
- Price, I.; Sanchez-Gonzalez, A.; Alet, F.; Andersson, T. R.; El-Kadi, A.; Masters, D.; Ewalds, T.; Stott, J.; Mohamed, S.; Battaglia, P.; Lam, R.; and Willson, M. 2025. Probabilistic weather forecasting with machine learning. *Nature*, 637(8044): 84–90.

- Ran, N.; Xiao, P.; Wang, Y.; Shi, W.; Lin, J.; Meng, Q.; and Allmendinger, R. 2024. Hr-extreme: A high-resolution dataset for extreme weather forecasting. *arXiv preprint arXiv:2409.18885*.
- Ravuri, S.; Lenc, K.; Willson, M.; Kangin, D.; Lam, R.; Mirowski, P.; Fitzsimons, M.; Athanassiadou, M.; Kashem, S.; Madge, S.; et al. 2021. Skilful precipitation nowcasting using deep generative models of radar. *Nature*, 597(7878): 672–677.
- Reichstein, M.; Benson, V.; Blunk, J.; Camps-Valls, G.; Creutzig, F.; Fearnley, C.; Han, B.; Kornhuber, K.; Rahaman, N.; Schölkopf, B.; et al. 2025. Early Warning of Complex Climate Risk with Integrated Artificial Intelligence. *Nature Communications*, 16(1): 2564.
- Stephenson, D. B.; Diaz, H. F.; and Murnane, R. J. 2008. Definition, Diagnosis, and Origin of Extreme Weather and Climate Events. *Climate Extremes and Society*, 340: 11–23.
- Veillette, M.; Samsi, S.; and Mattioli, C. 2020. Sevir: A storm event imagery dataset for deep learning applications in radar and satellite meteorology. *Advances in Neural Information Processing Systems*, 33: 22009–22019.
- Wang, F.; Chen, M.; He, X.; Zhang, Y.; Liu, F.; Guo, Z.; Hu, Z.; Wang, J.; Xu, J.; Li, Z.; et al. 2025a. OmniEarth-Bench: Towards Holistic Evaluation of Earth’s Six Spheres and Cross-Spheres Interactions with Multimodal Observational Earth Data. *arXiv preprint arXiv:2505.23522*.
- Wang, G.; Liu, Y.; Liu, S.; Zhang, L.; and Yang, L. 2025b. REMFLOW: RAG-Enhanced Multi-Factor Rainfall Flooding Warning in Sponge Airports via Large Language Model. *International Journal of Machine Learning and Cybernetics*, 1–21.
- Wu, H.; Zhou, H.; Long, M.; and Wang, J. 2023. Interpretable weather forecasting for worldwide stations with a unified deep model. *Nature Machine Intelligence*, 5(6): 602–611.
- Xiao, Y.; Bai, L.; Xue, W.; Chen, H.; Chen, K.; Han, T.; Ouyang, W.; et al. 2023. Towards a self-contained data-driven global weather forecasting framework. In *Forty-first International Conference on Machine Learning*.
- Zhang, Y.; Li, B.; Liu, H.; Lee, Y.; Gui, L.; Fu, D.; Feng, J.; Liu, Z.; and Li, C. 2024. LLaVA-NeXT: A Strong Zero-shot Video Understanding Model. <https://llava-vl.github.io/blog/2024-04-30-llava-next-video/>. Accessed: 2024-04-30.

Appendix

Meteorological Variables

In this study, to investigate the impact of atmospheric physical processes in the near-surface layer, troposphere, and stratosphere on warning issuance, we selected five key variables from the ERA5 reanalysis dataset across 37 vertical pressure levels (Table 2). Specifically, the 800–1000 hPa range represents the near-surface layer, 200–800 hPa corresponds to the main troposphere, and levels below 200 hPa are associated with the stratosphere

Variable	Definition	Unit	Pressure Levels (hPa)
z	geopotential	gpm	1, 2, 3, 5, 7, 10, 20, 30, 50, 70, 100,
u	U-component Wind Speed	m/s	125, 150, 175, 200, 225, 250, 300, 350,
v	V-component Wind Speed	m/s	400, 450, 500, 550, 600, 650, 700, 750,
t	Temperature	K	775, 800, 825, 850, 875, 900, 925, 950,
q	Specific Humidity	kg/kg	975, 1000

Table 1: Summary of the 5 physical variables in the dataset.

QA Types

Multiple Choice Question

As a professional meteorologist, please identify the severe weather events that occurred in **Beijing (Coordinates:[39.90°N,116.40°E])** based on the input data. Please select only one applicable option from the following options:

[Rain Storm]
A1: Blue-level A2: Yellow-level A3: Orange-level A4: Red-level

[Snow Storm]
B1: Blue-level B2: Yellow-level B3: Orange-level B4: Red-level

[Gale]
C1: Blue-level C2: Yellow-level C3: Orange-level C4: Red-level

[Cold Wave]
D1: Blue-level D2: Yellow-level D3: Orange-level D4: Red-level

[Heat Wave]
E1: Yellow-level E2: Orange-level E3: Red-level

[Frost]
F1: Blue-level F2: Yellow-level F3: Orange-level

[Hail]
G1: Orange-level G2: Red-level

[Normal Conditions]
H1: No warnings issued

Figure 1: An example of multiple choice question prompt for training and testing.

Binary Classification Question

As a professional meteorologist, please analyze the provided ERA5 dataset and determine whether **Maqu County (Coordinates: [34.00°N, 102.07°E])** is currently experiencing severe weather. Respond with either **”Yes”** or **”No”**.

Figure 2: An example of binary classification question prompt for training and testing.

Region-SW Question

As a professional meteorologist, please analyze the provided ERA5 data and assess the likelihood of severe weather events occurring in **Fuzhou City (Coordinates: [26.08°N, 119.30°E])**. Please identify which types of severe weather events may occur, selecting from the following categories:

Rain Storm, Snow Storm, Gale, Cold Wave, Heat Wave, Frost, Hail.

Figure 3: An example of Region-SW question prompt for training and testing.

National-SW Question

As a professional meteorologist, you are tasked with analyzing the provided dataset to identify and characterize any severe weather events that have occurred across **China’s** administrative divisions.

Please focus on the following regions with their respective coordinates:

Hebei(Coordinates:[38.04°N,114.51°E]), Shanxi(Coordinates:[37.87°N,112.55°E]), Liaoning(Coordinates:[41.80°N,123.50°E]), Jilin(Coordinates:[43.90°N,125.33°E]), Heilongjiang(Coordinates:[45.76°N,126.64°E]),.....

Determine what kind of severe weather occurred in each region. Output only the area where severe weather occurs For each detected event, use the following structured format: [Region Name] issues a [Event Type] [Severity Level].

Definitions:

1. Region Name (Administrative Divisions)
2. Event Type (Rain Storm/Snow Storm/Gale/Cold Wave/Heat Wave/Frost/Hail)
3. Severity Level (Blue/Yellow/Orange/Red)

Figure 4: An example of Nation-SW question prompt for training and testing.

COE

Fig. 5 shows contour plots of correct samples (blue) versus incorrect samples (red) across the two attention-feature dimensions—magnitude and angle—for all three QA tasks. The peak of the incorrect-sample distribution is shifted toward higher magnitude and angle values compared to the correct-sample distribution, and its contours are more dispersed, indicating that the meteorological features the model attends to when it errs are more complex and variable.

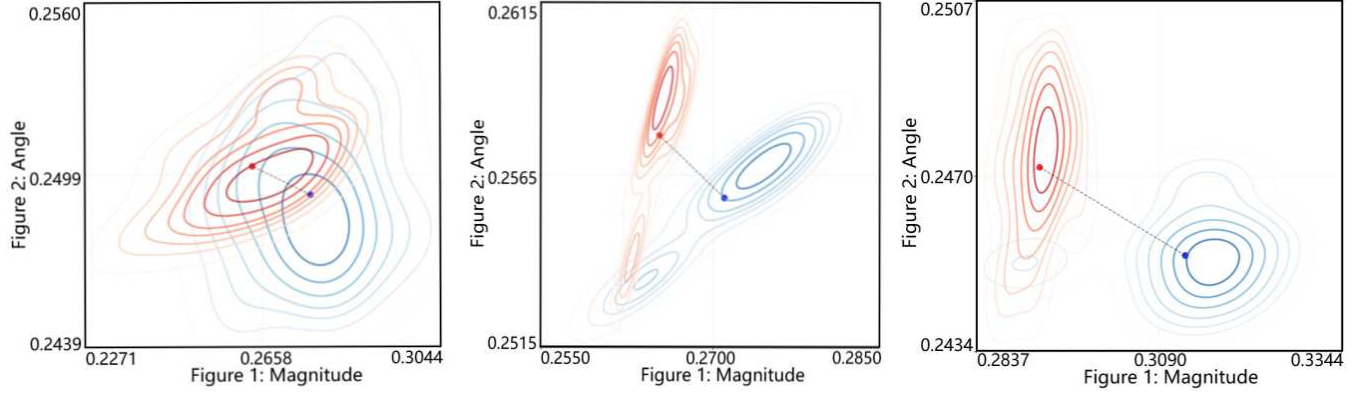


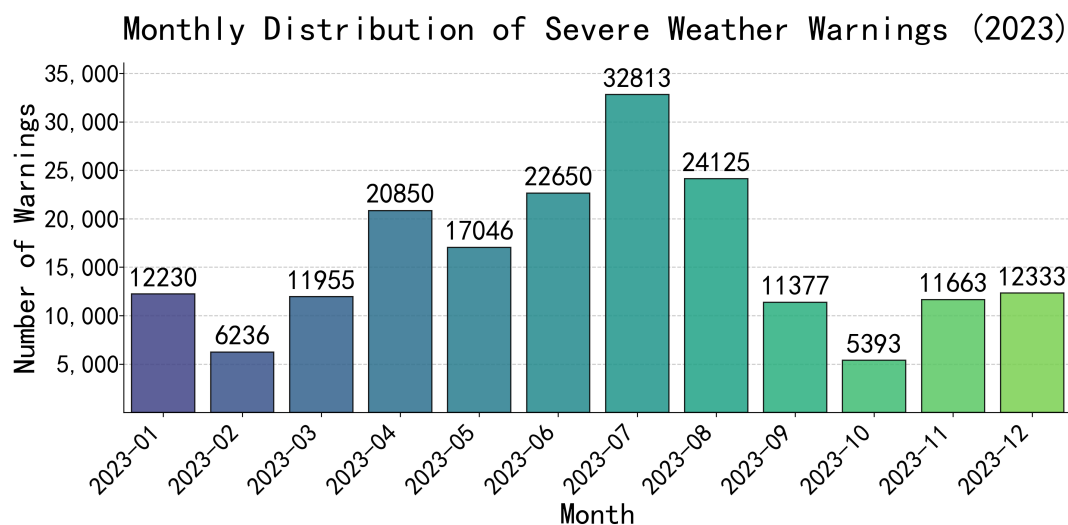
Figure 5: CoE Feature distribution of correct and incorrect sample sets in three Question types: (a) MC questions, (b) T/F questions, (c) RSW questions. Blue and Red distributions represent the correct and incorrect samples. Dataset used in this figure is testing set and model used in the figure is Qwen2.5-VL-7B-Instruct.

Severe Weather Warnings Text Dataset

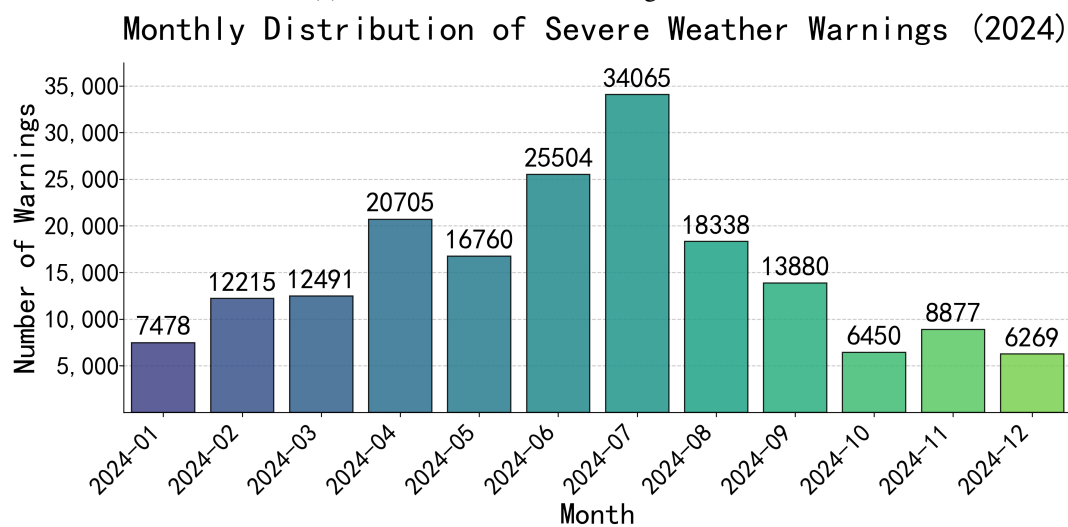
Table 1 presents the distribution of meteorological warning types for 2023–2024. Gale warnings account for the highest proportion (40%), snow storm warnings constitute the lowest (< 2%). Monthly warning distributions (Fig. 6) reveal peak issuance in July and minimal activity in October.

Year	Type	Num	Ratio (%)
2023	Gale	92939	43.54
	Rain Storm	47470	22.24
	Heat Wave	20787	09.74
	Cold Wave	11306	05.30
	Frost	7171	03.36
	Hail	5794	02.71
	Snow Storm	3204	01.50
	Normal	24810	11.62
	All	213481	100.0
2024	Gale	86314	41.52
	Rain Storm	48870	23.50
	Heat Wave	24767	11.91
	Cold Wave	8200	03.94
	Hail	7004	03.37
	Frost	4410	02.12
	Snow Storm	3467	01.67
	Normal	24850	11.95
	All	207882	100.0

Table 2: Statistics of severe weather warnings (2023-2024).



(a) 2023 severe weather warnings bar chart.



(b) 2024 severe weather warnings bar chart.

Figure 6: Monthly bar charts of severe weather warnings for the years (a) 2023 and (b) 2024.

GPT-4o's scoring criterion

You are a meteorological researcher. Your task is to compare the reference (ground-truth) answers with the outputs from a multi-modal meteorological model, assign a score from 0 to 5, and explain your reasoning. Each answer consists of multiple warning entries separated by commas, each formatted as: <Location><Level><Category>. Categories (8 types): Rain Storm, Snow Storm, Gale, Frost, Cold Wave, Heat Wave, Fog No Severe Weather. Levels (4 colors): Blue, Yellow, Orange, Red. Use the following open-ended scoring rubric (0-5) and explain why you chose that score:

5 – Completely accurate:

- All locations match exactly.
- For each warning, Level and Category both match perfectly.

4 – Accurate but slightly incomplete:

- Locations match exactly.
- Categories match perfectly; Levels partially match.

3 – Partially accurate:

- Most locations match, with minor omissions or discrepancies.
- Categories partially match; Levels partially match.

2 – Contains some errors:

- Some reference locations are missing in the model output.
- Categories partially match; Levels partially match.

1 – Mostly incorrect:

- Most reference locations are missing or incorrect.
- Only a small fraction of entries match in Location, Level, or Category.

0 – Completely incorrect or irrelevant:

- No locations match.
- No entries match in Level or Category.

Please score the following:

Standard answer: [Insert standard answer here]

Multimodal meteorological foundation model: [Insert student's answer here]

Please score the model's output according to the criteria and explain the reasoning for the score given.

Figure 7: GPT-4o's scoring criterion.

Detailed Experiment Setting

We employ LLaMA-Factory for model training and evaluation. Hyperparameters modified within the LLaMA-Factory framework are reported in Table 3 for each model, while all other hyperparameters retain their platform-default settings. Note that only intentionally adjusted hyperparameters are enumerated; all remaining configurations adhere strictly to LLaMA-Factory’s implementation defaults.

Weight Distribution Patterns of Plug-and-Play Modules

To determine the most sensitive pressure levels for five meteorological variables in the ERA5 dataset, we selected seven typical severe weather types (10 samples each) and analyzed them by calculating the average weights across all pressure levels. As shown in Fig. 8, the humidity variable exhibits peak sensitivity at 950 hPa, the geopotential height variable at 150 hPa, the U-component of wind at 350 hPa, the V-component of wind at 125 hPa, and the temperature variable at 100 hPa. This finding reveals characteristic vertical sensitivity patterns of atmospheric variables in severe weather scenarios, enhancing the interpretability of warning models. By identifying key physical layers—such as the 950 hPa level for moisture transport and the 150 hPa level for upper-level circulation—operators can trace the physical basis of model decisions, thereby improving the credibility and operational utility of warning systems.

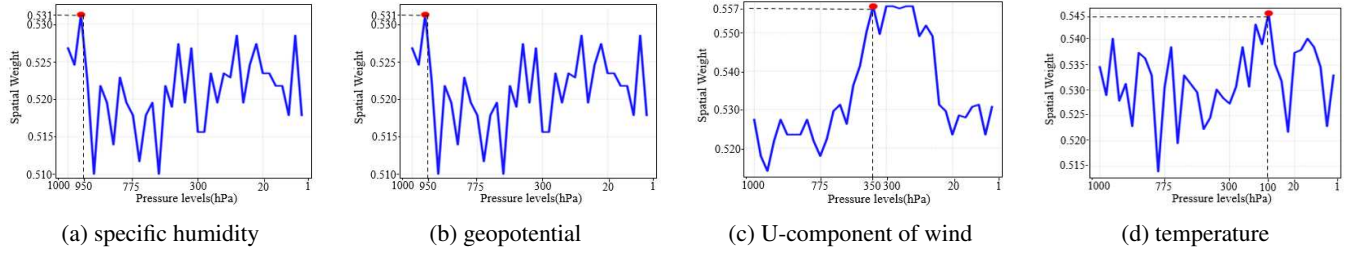


Figure 8: Examples of TGCA’s Weight distribution patterns. Each subplot represents a type of severe weather event.

Fig. 9 presents the hourly weight distributions of seven types of severe weather and normal weather samples processed by the DTGF module. Analysis shows that fluctuations in the temporal weights for normal weather are significantly lower than those for severe weather samples, reflecting a more stable evolution of meteorological variables—which aligns with the physical characteristic of normal weather processes lacking drastic phase transitions in atmospheric states. Further analysis in conjunction with Fig. 9 (a)-(g) reveals that red warning events exhibit higher weight values than blue warning events during the first three hours after issuance, confirming that the key meteorological variables associated with red warnings have higher variability during this period, a result consistent with theoretical expectations (Chen et al. 2020; Emanuel 1994; European Centre for Medium-Range Weather Forecasts 2021).

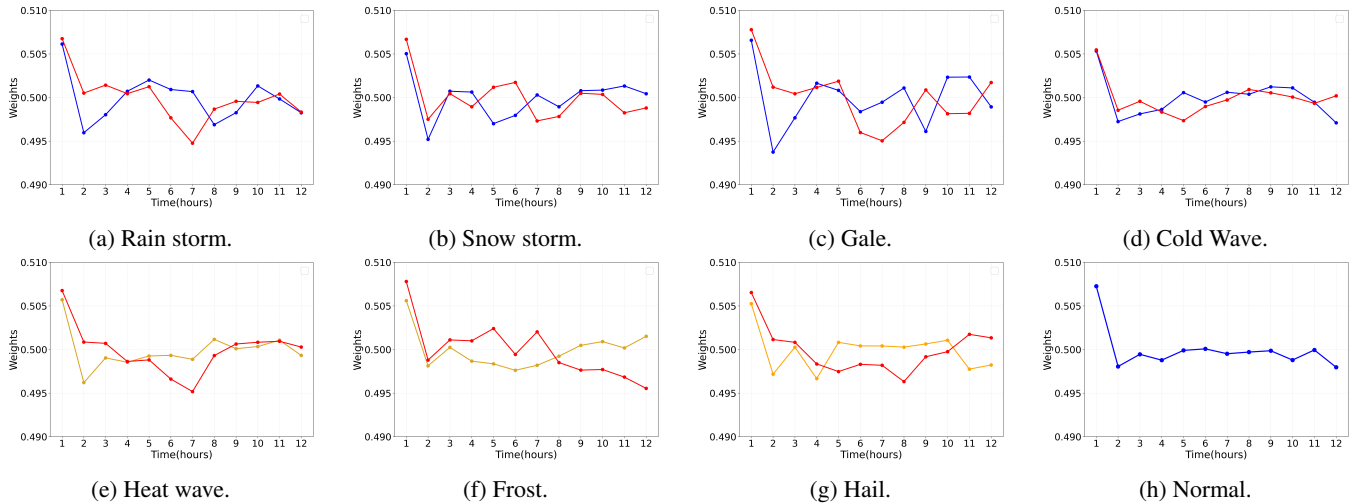


Figure 9: Examples of DTGF’s Weight distribution patterns. Each subplot represents a type of severe weather event. The red line indicates the most severe warning (red warning), while blue, yellow, and orange lines correspond to the lowest warning levels (blue, yellow, and orange warnings).

Parameter	Training	Evaluation
Model Parameters		
model_name_or_path	/model_pre-trained_weights	/model_pre-trained_weights
adapter_name_or_path	-	/lora-trained_weights
trust_remote_code	true	true
Method Parameters		
stage	sft	sft
do_train	True	False
finetuning_type	lora	lora
quantization_method	bitsandbytes	bitsandbytes
template	specific_model_templates	specific_model_templates
flash_attn	auto	auto
dataset_dir	-	data
dataset	train_data	-
eval_dataset	-	test_data
cutoff_len	9500	9500
max_samples	220000	100000
preprocessing_num_workers	16	16
LoRA Parameters		
lora_rank	8	-
lora_alpha	16	-
lora_dropout	0	-
lora_target	all	-
additional_target	gating_mlp, linear, text_proj, mlp_channel	-
Training Parameters		
per_device_train_batch_size	2	-
gradient_accumulation_steps	8	-
learning_rate	0.00005	-
num_train_epochs	3.0	-
lr_scheduler_type	cosine	-
max_grad_norm	1.0	-
warmup_steps	0	-
packing	False	-
report_to	none	-
bf16	True	-
optim	adamw_torch	-
ddp_timeout	180000000	-
include_num_input_tokens_seen	True	-
ddp_find_unused_parameters	False	-
Evaluation Parameters		
per_device_eval_batch_size	-	4
predict_with_generate	-	True
max_new_tokens	-	512
top_p	-	0.7
temperature	-	0.95
do_predict	-	True
Output Parameters		
output_dir	/path/to/outputs	/path/to/output
logging_steps	8	-
save_steps	200	-
plot_loss	True	-
overwrite_output_dir	True	-
save_only_model	False	-

Table 3: Model training and evaluation parameters.

References

- Chen, F.; Wang, Y.; Xue, M.; and Zhang, F. 2020. Rapid intensification of convective systems under red alerts. *Monthly Weather Review*, 148(5): 1897–1915.
- Emanuel, K. A. 1994. *Atmospheric convection*. New York: Oxford University Press. ISBN 9780195066303.
- European Centre for Medium-Range Weather Forecasts. 2021. Verification of severe weather warnings. Technical Memorandum 882, ECMWF.